

# Budget-Aware Graph Convolutional Network Design using Probabilistic Magnitude Pruning

Hichem Sahbi  
Sorbonne University, UPMC, CNRS, LIP6, France

---

◆

---

## Abstract

Graph convolutional networks (GCNs) are nowadays becoming mainstream in solving many image processing tasks including skeleton-based recognition. Their general recipe consists in learning convolutional and attention layers that maximize classification performances. With multi-head attention, GCNs are highly accurate but oversized, and their deployment on edge devices requires their pruning. Among existing methods, magnitude pruning (MP) is relatively effective but its design is clearly suboptimal as network topology selection and weight retraining are achieved independently.

In this paper, we devise a novel lightweight GCN design dubbed as Probabilistic Magnitude Pruning (PMP) that jointly trains network topology and weights. Our method is variational and proceeds by aligning the weight distribution of the learned networks with an a priori distribution. This allows implementing any fixed pruning rate, and also enhancing the generalization performances of the designed lightweight GCNs. Extensive experiments conducted on the challenging task of skeleton-based recognition show a substantial gain of our lightweight GCNs particularly at very high pruning regimes.

**Keywords.** Graph convolutional networks, lightweight design, magnitude pruning, skeleton-based recognition

## 1 INTRODUCTION

With the resurgence of deep neural networks [23], many image processing and pattern recognition tasks have been successfully revisited during the last decade [25]–[27], [30]. These tasks have been approached with increasingly accurate but *oversized* networks, and this makes their deployment on cheap devices, endowed with limited hardware resources, highly challenging. Among existing models, graph convolutional networks (GCNs) are known to be effective particularly on non-euclidean domains including point-clouds and skeletons [9], [29]. Two categories of GCNs are known in the literature; spatial and spectral. Spectral methods [32]–[34], [36]–[38] first project graph signals from the input to the Fourier domain in order to achieve convolution [46], and then back-project the convolved signals in the input domain. Spatial methods [40], [42]–[44] proceed differently by aggregating node signals using attention mechanisms prior to apply convolutions on the resulting node aggregates [47]. Spatial GCNs are deemed more effective compared to spectral ones, but their main downside resides in the high computational complexity especially when using multi-head attention.

A major challenge in deep learning is how to make these networks lightweight and frugal while maintaining their high accuracy [49], [51], [52], [54]. In this regard, many existing works tackle the issue of lightweight network design including tensor decomposition [73], quantization [68], distillation [55], [57]–[59], [61], [62] and pruning [64], [65], [67]. In particular, pruning methods are highly effective. Their principle consists in removing connections whose impact on the classification performances is the least noticeable. Two major categories of pruning techniques exist in the literature; structured [70], [72] and unstructured [67], [68]. The former consists in

zeroing-out weights of entire filters or channels whilst the latter seeks to remove weights individually and independently. Whereas structured methods produce computationally more efficient networks, they are less effective compared to unstructured techniques; indeed, the latter provide more flexible (and thereby more accurate) networks which are computationally still efficient.

Magnitude pruning (MP) is one of the mainstream methods that proceeds by removing the smallest weight connections in a given heavy network, prior to retrain the resulting pruned (lightweight) network. While being able to reach any targeted pruning rate, MP is clearly sub-optimal as its design *decouples* the training of network topology from weights. Therefore, any removed connection cannot be recovered when retraining the pruned network, and this usually leads to a significant drop in classification performances. In this paper, we investigate a novel alternative for magnitude pruning referred to as PMP (Probabilistic Magnitude Pruning) that allows *coupling* the training of network topology and weights. The proposed method constrains the distribution of the learned weights to match any arbitrary targeted distribution and this allows, *via a band-stop mechanism*, to filter out all the connections up to a given targeted pruning rate. Hence, the advantage of the proposed contribution is twofold; on the one hand, it allows reaching any pruning rate almost exactly, and on the other hand, it constrains the learned weights to fit a targeted distribution and this leads to better generalization as reported in experiments.

## 2 GRAPH CONVNETS AT A GLANCE

Let  $\mathcal{S} = \{\mathcal{G}_i = (\mathcal{V}_i, \mathcal{E}_i)\}_i$  denote a collection of graphs with  $\mathcal{V}_i, \mathcal{E}_i$  being respectively the nodes and the edges of  $\mathcal{G}_i$ . Each graph  $\mathcal{G}_i$  (denoted for short as  $\mathcal{G} = (\mathcal{V}, \mathcal{E})$ ) is endowed with a signal  $\{\phi(u) \in \mathbb{R}^s : u \in \mathcal{V}\}$  and associated with an adjacency matrix  $\mathbf{A}$ . GCNs aim at learning a set of  $C$  filters  $\mathcal{F}$  that define convolution on  $n$  nodes of  $\mathcal{G}$  (with  $n = |\mathcal{V}|$ ) as  $(\mathcal{G} \star \mathcal{F})_{\mathcal{V}} = f(\mathbf{A} \mathbf{U}^{\top} \mathbf{W})$ , here  $\top$  stands for transpose,  $\mathbf{U} \in \mathbb{R}^{s \times n}$  is the graph signal,  $\mathbf{W} \in \mathbb{R}^{s \times C}$  is the matrix of convolutional parameters corresponding to the  $C$  filters and  $f(\cdot)$  is a nonlinear activation applied entry-wise. In  $(\mathcal{G} \star \mathcal{F})_{\mathcal{V}}$ , the input signal  $\mathbf{U}$  is projected using  $\mathbf{A}$  and this provides for each node  $u$ , the aggregate set of its neighbors. Entries of  $\mathbf{A}$  could be handcrafted or learned so  $(\mathcal{G} \star \mathcal{F})_{\mathcal{V}}$  makes it possible to implement a convolutional block with two layers; the first one aggregates signals in  $\mathcal{N}(\mathcal{V})$  (sets of node neighbors) by multiplying  $\mathbf{U}$  with  $\mathbf{A}$  while the second layer achieves convolution by multiplying the resulting aggregates with the  $C$  filters in  $\mathbf{W}$ . Learning multiple adjacency (also referred to as attention) matrices (denoted as  $\{\mathbf{A}^k\}_{k=1}^K$ ) allows us to capture different contexts and graph topologies when achieving aggregation and convolution. With multiple matrices  $\{\mathbf{A}^k\}_k$  (and associated convolutional filter parameters  $\{\mathbf{W}^k\}_k$ ),  $(\mathcal{G} \star \mathcal{F})_{\mathcal{V}}$  is updated as  $f(\sum_{k=1}^K \mathbf{A}^k \mathbf{U}^{\top} \mathbf{W}^k)$ . Stacking aggregation and convolutional layers, with multiple matrices  $\{\mathbf{A}^k\}_k$ , makes GCNs accurate but heavy. We propose, in what follows, a method that makes our networks lightweight and still effective.

## 3 LIGHTWEIGHT GCN DESIGN

In the remainder of this paper, we subsume a given GCN as a multi-layered neural network  $g_{\theta}$  whose weights are defined as  $\theta = \{\mathbf{W}^1, \dots, \mathbf{W}^L\}$ , with  $L$  being its depth,  $\mathbf{W}^{\ell} \in \mathbb{R}^{d_{\ell-1} \times d_{\ell}}$  its  $\ell^{\text{th}}$  layer weight tensor, and  $d_{\ell}$  the dimension of  $\ell$ . The output of a given layer  $\ell$  is defined as  $\phi^{\ell} = f_{\ell}(\mathbf{W}^{\ell \top} \phi^{\ell-1})$ ,  $\ell \in \{2, \dots, L\}$ , being  $f_{\ell}$  an activation function; without a loss of generality, we omit the bias in the definition of  $\phi^{\ell}$ .

Pruning consists in zeroing-out a subset of weights in  $\theta$  by multiplying  $\mathbf{W}^{\ell}$  with a binary mask  $\mathbf{M}^{\ell} \in \{0, 1\}^{d_{\ell-1} \times d_{\ell}}$ . The binary entries of  $\mathbf{M}^{\ell}$  are set depending on whether the underlying layer connections are kept or removed, so  $\phi^{\ell} = f_{\ell}((\mathbf{M}^{\ell} \odot \mathbf{W}^{\ell})^{\top} \phi^{\ell-1})$ , here  $\odot$  stands for the element-wise matrix product. In this definition, entries of the tensor  $\{\mathbf{M}^{\ell}\}_{\ell}$  are set depending on the prominence

of the underlying connections in  $g_\theta$ . However, such pruning suffers from several drawbacks. On the one hand, optimizing the discrete set of variables  $\{\mathbf{M}^\ell\}_\ell$  is known to be highly combinatorial and intractable especially on large networks. On the other hand, the total number of parameters  $\{\mathbf{M}^\ell\}_\ell, \{\mathbf{W}^\ell\}_\ell$  is twice the number of connections in  $g_\theta$  and this increases training complexity and may also lead to overfitting.

### 3.1 Band-stop Weight Parametrization

In order to circumvent the above issues, we consider an alternative *parametrization*, related to magnitude pruning, that allows finding both the topology of the pruned networks together with their weights, without doubling the size of the training parameters, while making learning still effective. This parametrization corresponds to the Hadamard product involving a weight tensor and a function applied entry-wise to the same tensor as

$$\mathbf{W}^\ell = \hat{\mathbf{W}}^\ell \odot \psi(\hat{\mathbf{W}}^\ell), \quad (1)$$

here  $\hat{\mathbf{W}}^\ell$  is a latent tensor and  $\psi(\hat{\mathbf{W}}^\ell)$  is a continuous relaxation of  $\mathbf{M}^\ell$  which enforces the prior that smallest weights should be removed from the network. In order to achieve this goal,  $\psi$  must be (i) bounded in  $[0, 1]$ , (ii) differentiable, (iii) symmetric, and (iv)  $\psi(\omega) \rightsquigarrow 1$  when  $|\omega|$  is sufficiently large and  $\psi(\omega) \rightsquigarrow 0$  otherwise. The first and the fourth properties ensure that the parametrization is neither acting as a scaling factor greater than one nor changing the sign of the latent weight, and also acts as the identity for sufficiently large weights, and as a contraction factor for small ones. The second property is necessary to ensure that  $\psi$  has computable gradient while the third condition guarantees that only the magnitudes of the latent weights matter. A possible choice, used in practice, that satisfies these four conditions is  $\psi_{a,\sigma}(\hat{\mathbf{w}}) = (1 + \sigma \exp(a^2 - \hat{\mathbf{w}}^2))^{-1}$  with  $\sigma$  being a scaling factor and  $a$  threshold. As shown in Fig. 1,  $(\sigma, a)$  control the smoothness of  $\psi_{a,\sigma}$  around the support  $\Omega \subseteq \mathbb{R}$  of the latent weights. This allow implementing an annealed (soft) thresholding function that cuts-off all the connections in smooth and differentiable manner as training of the latent parameters evolves. Put differently, the asymptotic behavior of  $\psi_{a,\sigma}$  — that allows selecting the topology of the pruned subnetworks — is obtained as training reaches the latest epochs.

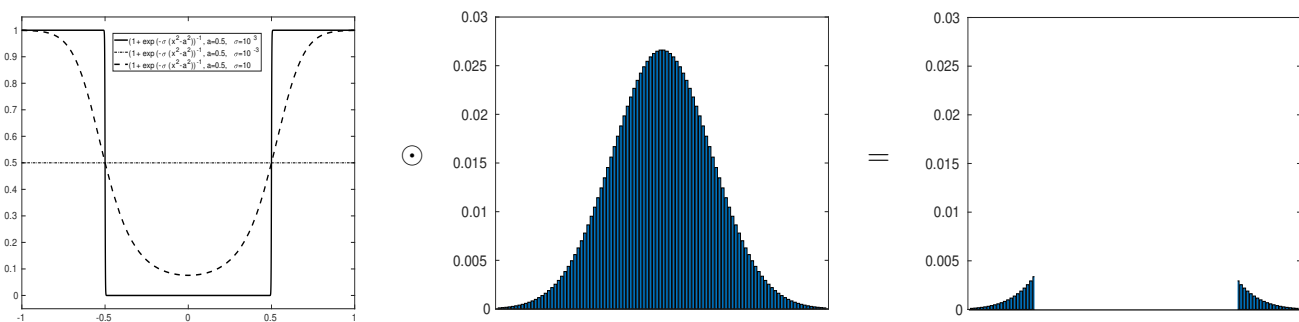


Fig. 1: This illustration shows a Band-stop function  $\psi_{a,\sigma}$  and its application to a given (gaussian) weight distribution. Depending on the setting of  $a$ , only large magnitude weights are kept and correspond to the fixed pruning rate. (Better to zoom the file).

### 3.2 Probabilistic Magnitude Pruning

The aforementioned parameterization — while being effective (see later experiments) — it does not allow to implement any targeted pruning rate as the dynamic of learned latent weights

$\{\hat{\mathbf{W}}^\ell\}_\ell$  is not known a priori. Hence, pruning rates could only be observed a posteriori or implemented after training using a two stage process (e.g., magnitude pruning + retraining). In order to implement any a priori targeted pruning rate as a part of a single training process, we constrain the distribution of latent weights to fit an arbitrary probability distribution, so one may fix  $a$  in  $\psi_{a,\sigma}$  and thereby achieve the targeted pruning rate. Let  $\hat{W} \in \Omega$  denote a random variable standing for the latent weights in the pruned network  $g_\theta$ ;  $\hat{W}$  is assumed drawn from any arbitrary distribution  $P$  (uniform, gaussian, laplace, etc). Fixing appropriately the distribution  $P$  *not only* allows implementing any targeted pruning rate, but has also a regularization effect which controls the dynamic of the learned weights and thereby the generalization properties of  $g_\theta$  as shown subsequently and later in experiments.

**Fitting a targeted distribution.** Considering  $Q$  as the observed distribution of the latent weights  $\{\hat{\mathbf{W}}^\ell\}_\ell$ , and  $P$  the targeted one, our goal is to reduce the discrepancy between  $P$  and  $Q$  using a Kullback-Leibler Divergence (KLD) loss

$$D_{KL}(P||Q) = \int_{\Omega} P(\hat{W})(\log P(\hat{W}) - \log Q(\hat{W})) d\hat{W}. \quad (2)$$

Note that the analytic form of the above equation is known on the widely used probability density functions (PDFs), whilst for general (arbitrary) probability distributions, the exact form is not always known and requires sampling. Hence, we consider instead a discrete variant of this loss as well as  $P$  and  $Q$ ; examples of discrete targeted distributions  $P$  are given in Fig. 2 while the observed (and also differentiable) one  $Q$  is based on a relaxed variant of histogram estimation. Let  $\{q_1, \dots, q_K\}$  denote a  $K$ -bin quantization of  $\Omega$  (in practice  $K = 100$ ), the  $k$ -th entry of  $Q$  is defined as

$$Q(\hat{W} = q_k) \propto \sum_{\ell=1}^{L-1} \sum_{i=1}^{n_\ell} \sum_{j=1}^{n_{\ell+1}} \exp \left\{ - (\hat{\mathbf{W}}_{i,j}^\ell - q_k)^2 / \beta_k^2 \right\}, \quad (3)$$

here  $\beta_k^2$  is a scaling factor that controls the smoothness of the exponential function; larger values of  $\beta_k$  result into oversmoothed histogram estimation while a sufficiently (not very) small  $\beta_k$  leads to a surrogate histogram estimation close to the actual discrete distribution of  $Q$ . In practice,  $\beta_k$  is set to  $(q_{k+1} - q_k)/2$ ; with this setting, one may replace  $\propto$  (in Eq. 3) with an equality as the partition function of  $Q$  — i.e.,  $\sum_{k=1}^K Q(\hat{W} = q_k)$  — reaches almost one in practice.

**Budget-aware pruning.** Let  $F_{\hat{W}}(a) = P(\hat{W} \leq a)$  be the cumulative distribution function (CDF) of  $P(\hat{W})$ . For any given pruning rate  $r$ , one may find the threshold  $a$  of the parametrization  $\psi_{a,\sigma}$  as

$$a = F_{\hat{W}}^{-1}(r). \quad (4)$$

The above function, known as the quantile, defines the pruning threshold  $a$  on the targeted distribution  $P$  (and equivalently on the observed one  $Q$  thanks to the KLD loss) which guarantees that only a fraction  $(1 - r)$  of the total weights are kept (i.e, nonzero) when applying the band-stop reparametrization in Eq. 1. Note that the quantile at any given pruning rate  $r$ , can either be empirically evaluated on discrete random variables or can be analytically derived on the widely used PDFs (see table. 1).

Considering the above budget implementation, pruning is achieved using a global loss as a combination of a cross-entropy term  $\mathcal{L}_e$ , and the KLD loss  $D_{KL}$  (which controls weight distribution and hence guarantees the targeted pruning rate/budget depending on the setting of  $a$  in  $\psi_{a,\sigma}$  as shown in Eq. 4) resulting into

$$\min_{\{\hat{\mathbf{W}}^\ell\}_\ell} \mathcal{L}_e(\{\hat{\mathbf{W}}^\ell \odot \psi(\hat{\mathbf{W}}^\ell)\}_\ell) + \lambda D_{KL}(P||Q), \quad (5)$$

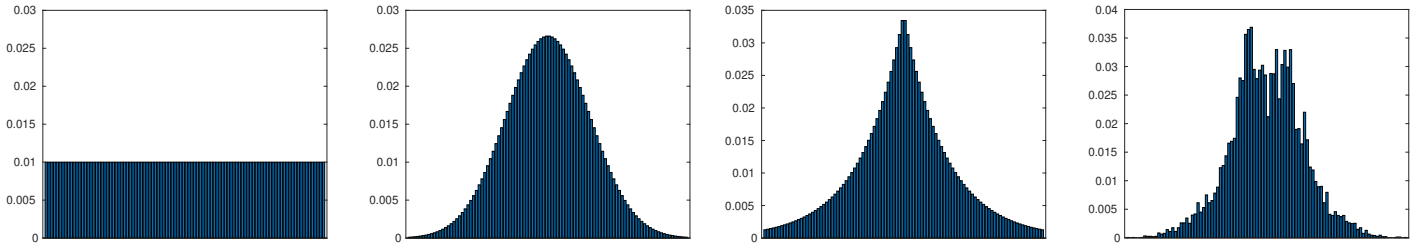


Fig. 2: The first 3 figures correspond to targeted (uniform, gaussian and laplace) distributions. The 4th figure shows the actual weight distribution of the heavy/unpruned GCN which resembles to gaussian. This may explain the best performances when the gaussian target is used particularly at low/mid pruning rates where the unpruned and pruned networks are more similar. At high pruning rates, laplace is better (see table 3).

here  $\lambda$  is sufficiently large (overestimated to  $\lambda = 10$  in practice), so Eq. 5 focuses on implementing the budget and also constraining the pruning rate to reach  $r$ . As training evolves,  $D_{KL}$  reaches its minimum and stabilizes while the gradient of the global loss becomes dominated by the gradient of  $\mathcal{L}_e$ , and this maximizes further the classification performances.

Note that the impact of  $D_{KL}(P||Q)$  in Eq. 5 has some similarities and differences w.r.t. the usual

Distributions	PDF $P(\hat{W})$	Quantile $a = F_{\hat{W}}^{-1}(r)$
Uniform	$\frac{1}{T}$	$a = \frac{r}{T}$
Gaussian	$\frac{1}{\sigma\sqrt{2\pi}} \exp \left\{ -\frac{1}{2} \left( \frac{\hat{W}-\mu}{\sigma} \right)^2 \right\}$	$a = \mu + \sigma\sqrt{2}\text{erf}^{-1}(2r - 1)$
Laplace	$\frac{1}{2b} \exp \left\{ -\frac{ \hat{W}-b }{b} \right\}$	$a = \begin{cases} \mu + b \log(2r) & \text{if } r \leq \frac{1}{2} \\ \mu - b \log(2 - 2r) & \text{otherwise} \end{cases}$

TABLE 1: Different standard PDFs and the underlying quantile functions.

regularizers particularly  $\ell_0$ ,  $\ell_1$  and  $\ell_2$ . Whilst these three regularizers favor respectively uniform, laplace and gaussian distributions in  $Q$ , there is no guarantee that  $Q$  will *exactly match* an a priori distribution, so implementing any targeted pruning rate will require adding explicit (and difficult to solve) budget criteria. In contrast, as  $Q$  is constrained in  $D_{KL}(P||Q)$ , the Band-pass mechanism in Eq. 1 makes reaching any targeted pruning rate easily feasible. Note also that this Band-pass mechanism allows implementing a *partial weight ranking* — through the  $K$ -bins of the distribution  $Q$  — in a differentiable manner. In other words, as training evolves, this approach jointly trains network topology  $\psi_{a,\sigma}(\hat{\mathbf{W}}^\ell)$  and weights  $\hat{\mathbf{W}}^\ell$  by (i) changing the *bin assignment* of  $\hat{\mathbf{W}}^\ell$  in  $Q$ , and by (ii) *activating and deactivating* these weights through  $\psi_{a,\sigma}$  while maximizing generalization and satisfying exactly the targeted budget.

## 4 EXPERIMENTS

We benchmark our GCNs on the task of action recognition using the First-Person Hand Action (FPHA) dataset [2] which includes 1175 skeletons belonging to 45 action categories. Each sequence of skeletons (video) is initially described with a graph  $\mathcal{G} = (\mathcal{V}, \mathcal{E})$  with each node  $v_j \in \mathcal{V}$  corresponding to the  $j$ -th hand-joint trajectory (denoted as  $\{\hat{p}_j^t\}_t$ ) and an edge  $(v_j, v_i) \in \mathcal{E}$  exists iff the  $j$ -th and the  $i$ -th trajectories are spatially connected. Each trajectory in  $\mathcal{G}$  is processed

Method	Color	Depth	Pose	Accuracy (%)
Two stream-color [4]	✓	✗	✗	61.56
Two stream-flow [4]	✓	✗	✗	69.91
Two stream-all [4]	✓	✗	✗	75.30
HOG2-depth [5]	✗	✓	✗	59.83
HOG2-depth+pose [5]	✗	✓	✓	66.78
HON4D [6]	✗	✓	✗	70.61
Novel View [7]	✗	✓	✗	69.21
1-layer LSTM [9]	✗	✗	✓	78.73
2-layer LSTM [9]	✗	✗	✓	80.14
Moving Pose [10]	✗	✗	✓	56.34
Lie Group [12]	✗	✗	✓	82.69
HBRNN [14]	✗	✗	✓	77.40
Gram Matrix [15]	✗	✗	✓	85.39
TF [18]	✗	✗	✓	80.69
JOULE-color [19]	✓	✗	✗	66.78
JOULE-depth [19]	✗	✓	✗	60.17
JOULE-pose [19]	✗	✗	✓	74.60
JOULE-all [19]	✓	✓	✓	78.78
Huang et al. [20]	✗	✗	✓	84.35
Huang et al. [22]	✗	✗	✓	77.57
Our GCN baseline	✗	✗	✓	<b>86.43</b>

TABLE 2: Comparison of our baseline GCN against related work on FPHA.

using *temporal chunking* [71]: first, the total duration of a sequence is split into  $M$  evenly-sized temporal chunks ( $M = 32$  in practice), then the trajectory coordinates  $\{\hat{p}_j^t\}_t$  are assigned to the  $M$  chunks (depending on their time stamps) prior to concatenate the averages of these chunks. This produces the raw description (signal) of  $v_j$ .

**Implementation details and baseline GCN.** We trained the GCNs end-to-end using the Adam optimizer [1] for 2,700 epochs with a batch size equal to 600, a momentum of 0.9 and a global learning rate (denoted as  $\nu(t)$ ) inversely proportional to the speed of change of our global loss used to train our networks. When this speed increases (resp. decreases),  $\nu(t)$  decreases as  $\nu(t) \leftarrow \nu(t-1) \times 0.99$  (resp. increases as  $\nu(t) \leftarrow \nu(t-1)/0.99$ ). We use in our experiments a GeForce GTX 1070 GPU (with 8 GB memory) and we evaluate the performances using the protocol proposed in [2] with 600 action sequences for training and 575 for testing, and we report the average accuracy over all the classes of actions. The architecture of our baseline GCN (taken from [71]; see also section 2) includes stacked 8-head attentions applied to skeleton graphs whose nodes are encoded with 16-channels, followed by convolutions of 32 filters, and a dense fully connected layer as well as a final classification layer. In total, this initial network is relatively heavy (for a GCN). Nevertheless, this GCN is accurate compared to the related work on the FPHA benchmark as shown in Table. 2. Considering this GCN baseline, our goal is to make it lightweight while maintaining its high accuracy.

**GCN performances.** Table 3 shows the performances of our baseline and lightweight GCNs. From these results, we observe the positive impact for different PDFs and for increasing pruning rates  $r$ ; for mid  $r$  values (i.e., 55%), MP+gaussian overtakes all the other setting while for very high

Fixed PR	Observed PR + gap	Target PDFs.	Accuracy (%)	Observation
none	0.00 (0.00)	✗	<b>86.43</b>	Baseline GCN (BGCN)
	0.00 (0.00)	✓	86.26	BGCN+Uniform
0%	0.00 (0.00)	✓	<b>86.60</b>	BGCN+Gaussian
	0.00 (0.00)	✓	86.26	BGCN+Laplace
55%	55.00 (0.00)	✗	87.82	MP
	55.10 (0.10)	✓	87.82	MP+Uniform
	55.31 (0.31)	✓	<b>88.52</b>	MP+Gaussian
	57.83 (2.83)	✓	87.65	MP+Laplace
80%	80.00 (0.00)	✗	86.78	MP
	77.74 (2.26)	✓	85.91	MP+Uniform
	80.71 (0.71)	✓	<b>87.47</b>	MP+Gaussian
	80.11 (0.11)	✓	86.95	MP+Laplace
98%	98.00 (0.00)	✗	60.34	MP
	97.98 (0.02)	✓	70.26	MP+Uniform
	97.97 (0.03)	✓	70.60	MP+Gaussian
	97.90 (0.10)	✓	<b>70.80</b>	MP+Laplace
99%	99.01 (0.01)	✗	46.26	MP
	98.67 (0.33)	✓	62.43	MP+Uniform
	98.72 (0.28)	✓	56.17	MP+Gaussian
	98.86 (0.14)	✓	<b>64.17</b>	MP+Laplace

TABLE 3: Detailed performances and ablation study, for different fixed and observed pruning rates, and for different targeted probability distributions. Here “PR” stands for pruning rate, and “gap” as the difference between fixed and observed pruning rates.

pruning regimes (i.e.,  $\geq 98\%$ ), MP+laplace is the most performant. Note that lightweight GCNs with mid  $r$  overtake the baseline; indeed, mid  $r$  values produce subnetworks with already enough (a large number of) connections and having some of them removed from the baseline GCNs produces a well known regularization effect [48]. We also note that the fixed and the observed pruning rates are very similar; the quantile functions of the gaussian and laplace PDFs allow implementing *fine-steps* of the targeted pruning rates particularly when  $r$  is large. In contrast, the quantile functions of the gaussian and laplace PDFs are coarse around mid  $r$  values (i.e., 55%).

## 5 CONCLUSION

We introduce in this paper a novel lightweight GCN design based on probabilistic magnitude pruning. The strength of the proposed method resides in its ability to constrain the probability distribution of the learned GCNs to match an a priori distribution and this allows implementing any given targeted pruning rate while also enhancing the generalization performances of the resulting GCNs. Experiments conducted on the challenging task of skeleton-based recognition shows a significant gain of our method. As a future work, we are currently investigating the extension of the current approach to other networks and databases.

## REFERENCES

- [1] D.P. Kingma, and J. Ba. “Adam: A method for stochastic optimization.” arXiv preprint arXiv:1412.6980 (2014)

- [2] G. Garcia-Hernando, S. Yuan, S. Baek, and T.-K. Kim. First- Person Hand Action Benchmark with RGB-D Videos and 3D Hand Pose Annotations. In CVPR, 2018
- [3] M. Jiu and H. Sahbi. "Laplacian deep kernel learning for image annotation." 2016 IEEE International Conference on Acoustics, Speech and Signal Processing (ICASSP). IEEE, 2016.
- [4] C. Feichtenhofer, A. P., and A. Zisserman. Convolutional Two-Stream Network Fusion for Video Action Recognition. CVPR, pages 1933-1941, 2016. 8
- [5] E.Ohn-Barand, M.M.Trivedi. Hand Gesture Recognition in Real Time for Automotive Interfaces: A Multimodal Vision- Based Approach and Evaluations. IEEE TITS, 15(6):2368–2377, 2014.
- [6] O. Oreifej and Z. Liu. HON4D: Histogram of Oriented 4D Normals for Activity Recognition from Depth Sequences. In CVPR, pages 716-723, June 2013.
- [7] H. Rahmani and A. Mian. 3D Action Recognition from Novel Viewpoints. In CVPR, pages 1506–1515, June 2016.
- [8] H. Sahbi, J.-Y. Audibert, and R. Keriven, "Context-dependent kernels for object classification," *IEEE Transactions on Pattern Analysis and Machine Intelligence*, vol. 33, pp. 699–708, 2011.
- [9] W. Zhu, C. Lan, J. Xing, W. Zeng, Y. Li, L. Shen, and X. Xie. Co-occurrence feature learning for skeleton based action recognition using regularized deep LSTM networks In AAAI, volume 2, page 6, 2016.
- [10] M. Zanfir, M. Leordeanu, and C. Sminchisescu. The Moving Pose: An Efficient 3D Kinematics Descriptor for Low-Latency Action Recognition and Detection. In ICCV, pages 2752–2759, 2013.
- [11] N. Bourdis, D. Marraud, and H. Sahbi, Spatio-temporal interaction for aerial video change detection, in IGARSS, 2012, pp. 2253–2256
- [12] R. Vemulapalli, F. Arrate, and R. Chellappa. Human action recognition by representing 3D skeletons as points in a Lie group. In IEEE CVPR, pages 588–595, 2014
- [13] M. Jiu and H. Sahbi, "Nonlinear deep kernel learning for image annotation," *IEEE Transactions on Image Processing*, vol. 26(4), 2017.
- [14] Y. Du, W. Wang, and L. Wang. Hierarchical recurrent neural network for skeleton based action recognition. In IEEE CVPR, pages 1110–1118, 2015.
- [15] X. Zhang, Y. Wang, M. Gou, M. Sznaiar, and O. Camps. Efficient Temporal Sequence Comparison and Classification Using Gram Matrix Embeddings on a Riemannian Manifold. In CVPR, pages 4498–4507, 2016
- [16] F. Fleuret and H. Sahbi. "Scale-invariance of support vector machines based on the triangular kernel." 3rd International Workshop on Statistical and Computational Theories of Vision. 2003.
- [17] H. Sahbi, "Lightweight Connectivity In Graph Convolutional Networks For Skeleton-Based Recognition." 2021 IEEE International Conference on Image Processing (ICIP). IEEE, 2021.
- [18] G. Garcia-Hernando and T.-K. Kim. Transition Forests: Learning Discriminative Temporal Transitions for Action Recognition. In CVPR, pages 407–415, 2017.
- [19] J. Hu, W. Zheng, J. Lai, and J. Zhang. Jointly Learning Heterogeneous Features for RGB-D Activity Recognition. In CVPR 2015
- [20] Z. Huang and L. V. Gool. A Riemannian Network for SPD Matrix Learning. In AAAI, pages 2036–2042, 2017
- [21] N. Boujemaa, F. Fleuret, V. Gouet, H. Sahbi (2004, January). Visual content extraction for automatic semantic annotation of video news. In the proceedings of the SPIE Conference, San Jose, CA (Vol. 6).
- [22] Z. Huang, J. Wu, and L. V. Gool. Building Deep Networks on Grassmann Manifolds. In AAAI, pages 3279–3286, 2018
- [23] A. Krizhevsky, I. Sutskever, and G. E. Hinton, "Imagenet classification with deep convolutional neural networks," in NIPS 2012.
- [24] H. Sahbi, L. Ballan, G. Serra, A. DelBimbo (2012). Context-dependent logo matching and recognition. *IEEE Transactions on Image Processing*, 22(3), 1018-1031.
- [25] K. He, X. Zhang, S. Ren, and J. Sun, "Deep residual learning for image recognition," in *CVPR*, 2016, pp. 770–778.
- [26] G. Huang, Z. Liu, L. v. d. Maaten, and K. Q. Weinberger, "Densely connected convolutional networks," in *CVPR*, 2017, pp. 2261–2269.
- [27] He, Kaiming, et al. "Mask r-cnn." *Proceedings of ICCV*, 2017.
- [28] M. Ferecatu and H. Sahbi. "TELECOMParisTech at ImageClefphoto 2008: Bi-Modal Text and Image Retrieval with Diversity Enhancement." *CLEF (Working Notes)*. 2008.
- [29] Zhang, Ziwei, Peng Cui, and Wenwu Zhu. "Deep learning on graphs: A survey." *IEEE TKDE* (2020).
- [30] O. Ronneberger, P. Fischer, and T. Brox. "U-net: Convolutional networks for biomedical image segmentation." *International Conference on Medical image computing and computer-assisted intervention*. Springer, 2015.
- [31] H. Sahbi. Coarse-to-fine deep kernel networks. *Proceedings of the IEEE International Conference on Computer Vision*, 1131-1139, 2017.
- [32] J. Bruna, W. Zaremba, A. Szlam, Y. LeCun. Spectral networks and locally connected networks on graphs. arXiv:1312.6203 (2013)
- [33] M. Henaff, J. Bruna, Y. LeCun. Deep convolutional networks on graph structured data. arXiv preprint arXiv:1506.05163 (2015)
- [34] TN. Kipf, M. Welling. Semi-supervised classification with graph convolutional networks. In *ICLR*, 2017
- [35] H. Sahbi. Kernel PCA for similarity invariant shape recognition. *Neurocomputing* 70 (16-18), 3034-3045
- [36] R. Levie, F. Monti, X. Bresson, M.M. Bronstein. Cayleynets: Graph convolutional neural networks with complex rational spectral filters. *IEEE Transactions on Signal Processing* 67(1), 97–109 (2018)



- [37] R. Li, S. Wang, F. Zhu, J. Huang. Adaptive graph convolutional neural networks. In AAAI, 2018.
- [38] M. Defferrard, X. Bresson, P. Vandergheynst. Convolutional Neural Networks on graphs with Fast Localized Spectral Filtering. In NIPS, 2016
- [39] H. Sahbi. "Kernel-based Graph Convolutional Networks." 2020 25th International Conference on Pattern Recognition (ICPR). IEEE, 2021.
- [40] M. Gori, G. Monfardini, F. Scarselli. A new model for learning in graph domains. In IEEE IJCNN, vol. 2, pp. 729–734, 2005.
- [41] S. Thiemert, H. Sahbi, and M. Steinebach, "Applying interest operators in semi-fragile video watermarking," in *Security, Steganography, and Watermarking of Multimedia Contents VII*, vol. 5681. International Society for Optics and Photonics, 2005, pp. 353–363.
- [42] A. Micheli. Neural network for graphs: A contextual constructive approach. IEEE TNN 20(3), 498-511 (2009)
- [43] Z. Wu, S. Pan, F. Chen, G. Long, C. Zhang, P.S. Yu. A comprehensive survey on graph neural networks. arXiv:1901.00596 (2019).
- [44] W. Hamilton, Z. Ying, J. Leskovec. Inductive representation learning on large graphs. In NIPS. pp. 1024–1034 (2017)
- [45] H. Sahbi. "Learning laplacians in chebyshev graph convolutional networks." Proceedings of the IEEE/CVF International Conference on Computer Vision. 2021.
- [46] Chung, Fan RK, and Fan Chung Graham. Spectral graph theory. No. 92. American Mathematical Soc., 1997.
- [47] Knyazev, Boris, Graham W. Taylor, and Mohamed Amer. "Understanding attention and generalization in graph neural networks." Advances in neural information processing systems 32 (2019).
- [48] Wan, Li, et al. "Regularization of neural networks using dropconnect." International conference on machine learning. PMLR, 2013.
- [49] Gao Huang, Shichen Liu, Laurens van der Maaten, and Kilian Q. Weinberger, "Condensenet: An efficient densenet using learned group convolutions," in *CVPR*, 2018.
- [50] A. Mazari and H. Sahbi. "MLGCN: Multi-Laplacian graph convolutional networks for human action recognition." The British Machine Vision Conference (BMVC). 2019.
- [51] M. Sandler, A. G. Howard, M. Zhu, A. Zhmoginov, and L.-C. Chen, "Mobilenetv2: Inverted residuals and linear bottlenecks," in *CVPR*, 2018.
- [52] A. G. Howard, M. Zhu, B. Chen, D. Kalenichenko, W. Wang, T. Weyand, M. Andreetto, and H. Adam, "Mobilenets: Efficient convolutional neural networks for mobile vision applications," *CoRR*, vol. abs/1704.04861, 2017.
- [53] H. Sahbi, "Imageclef annotation with explicit context-aware kernel maps," *International Journal of Multimedia Information Retrieval*, pp. 113–128, 2015.
- [54] M. Tan and Q. V. Le, "Efficientnet: Rethinking model scaling for convolutional neural networks," in *ICML*. 2019, vol. 97, PMLR.
- [55] G. E. Hinton, O. Vinyals, and J. Dean, "Distilling the knowledge in a neural network," *CoRR*, vol. abs/1503.02531, 2015.
- [56] S. Tollari, P. Mulhem, M. Ferecatu, H. Glotin, M. Detyniecki, P. Gallinari, H. Sahbi and Z-Q. Zhao. "A comparative study of diversity methods for hybrid text and image retrieval approaches." In Workshop of the Cross-Language Evaluation Forum for European Languages, pp. 585-592. Springer, Berlin, Heidelberg, 2008.
- [57] S. Zagoruyko and N. Komodakis, "Paying more attention to attention: Improving the performance of convolutional neural networks via attention transfer," in *ICLR*, 2017.
- [58] A. Romero, N. Ballas, S. Ebrahimi Kahou, A. Chassang, C. Gatta, and Y. Bengio, "Fitnets: Hints for thin deep nets," in *ICLR*, 2015.
- [59] S.-I. Mirzadeh, M. Farajtabar, A. Li, N. Levine, A. Matsukawa, and H. Ghasemzadeh, "Improved knowledge distillation via teacher assistant," in *AAAI*, 2020.
- [60] H. Sahbi and N. Boujemaa. "Coarse-to-fine support vector classifiers for face detection." Object recognition supported by user interaction for service robots. Vol. 3. IEEE, 2002.
- [61] Y. Zhang, T. Xiang, T. M. Hospedales, and H. Lu, "Deep mutual learning," in *CVPR*, 2018.
- [62] S. Ahn, S. X. Hu, A. C. Damianou, N. D. Lawrence, and Z. Dai, "Variational information distillation for knowledge transfer," in *CVPR*, 2019.
- [63] H. Sahbi, Coarse-to-fine support vector machines for hierarchical face detection. Diss. PhD thesis, Versailles University, 2003.
- [64] Y. LeCun, J. S. Denker, and S. A. Solla, "Optimal brain damage," in *NIPS*, 1989.
- [65] B. Hassibi and D. G. Stork, "Second order derivatives for network pruning: Optimal brain surgeon," in *NIPS*, 1992.
- [66] H. Sahbi, D. Geman. A hierarchy of support vector machines for pattern detection. Journal of Machine Learning Research 7.Oct (2006): 2087-2123.
- [67] S. Han, J. Pool, J. Tran, and W. J. Dally, "Learning both weights and connections for efficient neural network," in *NIPS*, 2015.
- [68] S. Han, H. Mao, and W. J. Dally, "Deep compression: Compressing deep neural network with pruning, trained quantization and huffman coding," in *ICLR*, 2016.
- [69] H. Sahbi and N. Boujemaa. "From coarse to fine skin and face detection." Proceedings of the eighth ACM international conference on Multimedia. 2000.
- [70] H. Li, A. Kadav, I. Durdanovic, H. Samet, and H. P. Graf, "Pruning filters for efficient convnets," in *ICLR*, 2017.
- [71] H. Sahbi. "Learning Connectivity with Graph Convolutional Networks." 25th ICPR. IEEE, 2021.
- [72] Z. Liu, J. Li, Z. Shen, G. Huang, S. Yan, and C. Zhang, "Learning efficient convolutional networks through network slimming," *ICCV*. 2017.

- [73] Howard, Andrew, et al. "Searching for mobilenetv3." ICCV 2019.
- [74] H. Sahbi. "CNRS-TELECOM ParisTech at ImageCLEF 2013 Scalable Concept Image Annotation Task: Winning Annotations with Context Dependent SVMs." CLEF (Working Notes). 2013.
- [75] B. Koneru, N. Girish, and V. Vasudevan. "Sparse artificial neural networks using a novel smoothed LASSO penalization." *IEEE TCS II: Express Briefs* 66.5 (2019): 848-852.
- [76] J. Tu, M. Liu, and H. Liu, "Skeleton-based human action recognition using spatial temporal 3d convolutional neural networks," in Proc. IEEE Int. Conf. Multimedia Expo (ICME), San Diego, CA, United states, Jul. 2018, pp. 1-6.
- [77] T. Stefan, H. Sahbi and M. Steinebach. "Using entropy for image and video authentication watermarks." *Security, Steganography, and Watermarking of Multimedia Contents VIII*. Vol. 6072. SPIE, 2006.
- [78] H. Liu, J. Tu, M. Liu, and R. Ding, "Learning explicit shape and motion evolution maps for skeleton-based human action recognition," in Proc. IEEE Int. Conf. Acoust. Speech Signal Process. (ICASSP), Calgary, AB, Canada, Apr. 2018, pp. 1333-1337.
- [79] Y. Ji, G. Ye, and H. Cheng. Interactive body part contrast mining for human interaction recognition. In *IEEE International Conference on Multimedia and Expo Workshop*, pages 1-6. IEEE, 2014.
- [80] W. Li, L. Wen, M. Choo Chuah, and S. Lyu. Category-blind human action recognition: A practical recognition system. In *IEEE International Conference on Computer Vision*, pages 4444-4452, 2015.
- [81] H. Sahbi, J.-Y. Audibert, R. Keriven. "Graph-cut transducers for relevance feedback in content based image retrieval." *2007 IEEE 11th International Conference on Computer Vision*. IEEE, 2007.
- [82] K. Yun, J. Honorio, D. Chattopadhyay, T.L. Berg, and D. Samaras. Two-person interaction detection using body pose features and multiple instance learning. In *IEEE Conference on Computer Vision and Pattern Recognition Workshop*, 2012.
- [83] Liu, Jianbo, Ying Wang, Shiming Xiang, and Chunhong Pan. "Han: An efficient hierarchical self-attention network for skeleton-based gesture recognition." *arXiv preprint arXiv:2106.13391* (2021).
- [84] T. Napoléon and H. Sahbi. "From 2D silhouettes to 3D object retrieval: contributions and benchmarking." *EURASIP Journal on Image and Video Processing* 2010 (2010): 1-17.
- [85] A. Kacem, M. Daoudi, B. Ben Amor, S. Berretti, J-Carlos. Alvarez-Paiva. A Novel Geometric Framework on Gram Matrix Trajectories for Human Behavior Understanding. *IEEE Transactions on Pattern Analysis and Machine Intelligence*, 28 September 2018
- [86] XS. Nguyen, L. Brun, O. Lezoray and S. Bougleux. A neural network based on SPD manifold learning for skeleton-based hand gesture recognition. In *IEEE International Conference on Computer Vision and Pattern Recognition, CVPR*, 2019.
- [87] Z. Huang, C. Wan, T. Probst, and L. V. Gool. Deep Learning on Lie Groups for Skeleton-Based Action Recognition. In *CVPR*, pages 6099-6108, 2017.
- [88] M. Jiu and H. Sahbi. "Context-aware deep kernel networks for image annotation." *Neurocomputing* 474 (2022): 154-167.
- [89] L. Shi, Y. Zhang, J. Cheng, and H. Lu. Non-Local Graph Convolutional Networks for Skeleton-Based Action Recognition. *CoRR*, abs/1805.07694, 2018
- [90] B. Li, X. Li, Z. Zhang, and F. Wu. Spatio-temporal graph routing for skeleton-based action recognition. *AAAI Conference on Artificial Intelligence*, 2019
- [91] H. Sahbi. "Topologically-Consistent Magnitude Pruning for Very Lightweight Graph Convolutional Networks." In *2022 IEEE International Conference on Image Processing (ICIP)*, pp. 3495-3499. IEEE, 2022.
- [92] T. Jiang, T. Huang and Y. Tian. Global Co-occurrence Feature Learning and Active Coordinate System Conversion for Skeleton-based Action Recognition. In *Winter Conference on Applications of Computer Vision*, pages 586-594. IEEE, 2020.
- [93] S. Yan, Y. Xiong, and D. Lin. Spatial Temporal Graph Convolutional Networks for Skeleton-Based Action Recognition. In *AAAI*, pages 7444-7452, 2018.
- [94] Y. Wen, L. Gao, H. Fu, F. Zhang, and S. Xia. Graph CNNs with motif and variable temporal block for skeleton-based action recognition. *AAAI Conference on Artificial Intelligence*, 2019.
- [95] H. Sahbi and H. Zhan. "FFNB: Forgetting-Free Neural Blocks for Deep Continual Learning." In *The British Machine Vision Conference (BMVC)*. 2021.
- [96] M. Liu and J. Yuan. Recognizing human actions as the evolution of pose estimation maps. In *IEEE Conference on Computer Vision and Pattern Recognition*, 2018.
- [97] M. Liu, H. Liu, and C. Chen. Enhanced Skeleton Visualization for View Invariant Human Action Recognition. *Pattern Recognition*, 68:346-362, 2017.
- [98] M. Jiu and H. Sahbi. "DHCN: Deep hierarchical context networks for image annotation." In *ICASSP 2021-2021 IEEE International Conference on Acoustics, Speech and Signal Processing (ICASSP)*, pp. 3810-3814. IEEE, 2021.
- [99] I. Lee, D. Kim, S. Kang, and S. Lee. Ensemble deep learning for skeleton-based action recognition using temporal sliding lstm networks. In *IEEE International Conference on Computer Vision*, pages 1012-1020, 2017.
- [100] S. Zhang, X. Liu, and J. Xiao. On geometric features for skeleton-based action recognition using multilayer lstm networks. In *Winter Conference on Applications of Computer Vision*, pages 148-157. IEEE, 2017
- [101] P. Zhang, C. Lan, J. Xing, W. Zeng, J. Xue, and N. Zheng. View adaptive recurrent neural networks for high performance human action recognition from skeleton data. *arXiv preprint arXiv:1703.08274*, 2017.
- [102] A. Mazari and H. Sahbi. "Coarse-to-fine aggregation for cross-granularity action recognition." In *2020 IEEE International Conference on Image Processing (ICIP)*, pp. 1541-1545. IEEE, 2020.
- [103] A. Shahroudy, J. Liu, T. T. Ng, and G. Wang. NTU RGB+D: A Large Scale Dataset for 3D Human Activity Analysis. In *CVPR*, pages 1010-1019, 2016.

- [104] J. Liu, G. Wang, P. Hu, L.-Y. Duan, and A. C. Kot. Global Context-Aware Attention LSTM Networks for 3D Action Recognition. In CVPR, pages 3671–3680, 2017.
- [105] M. Jiu and H. Sahbi. "Deep representation design from deep kernel networks." *Pattern Recognition* 88 (2019): 447-457.
- [106] H. Wang and L. Wang. Modeling Temporal Dynamics and Spatial Configurations of Actions Using Two-Stream Recurrent Neural Networks. CVPR, pages 3633–3642, 2017.
- [107] J. C. Nez, R. Cabido, J. J. Pantrigo, A. S. Montemayor, and J. F. Vlez. Convolutional Neural Networks and Long Short-Term Memory for Skeleton-based Human Activity and Hand Gesture Recognition. *Pattern Recognition*, 76(C):80–94, 2018.
- [108] H. Sahbi. "Deep total variation support vector networks." In Proceedings of the IEEE/CVF International Conference on Computer Vision Workshops, pp. 0-0. 2019.
- [109] P. Wang, Z. Li, Y. Hou, and W. Li. Action Recognition Based on Joint Trajectory Maps Using Convolutional Neural Networks. In ACM MM, pages 102–106, 2016.
- [110] Q. Ke, M. Bennamoun, S. An, F. Sohel, and F. Boussaid. A new representation of skeleton sequences for 3D action recognition. In IEEE Conference on Computer Vision and Pattern Recognition Workshop, pages 4570–4579. IEEE, 2017.
- [111] Q. Oliveau and H. Sahbi. "From transductive to inductive semi-supervised attributes for ship category recognition." In IGARSS 2018-2018 IEEE International Geoscience and Remote Sensing Symposium, pp. 4827-4830. IEEE, 2018.
- [112] X. Chen, H. Guo, G. Wang, and L. Zhang, "Motion feature augmented recurrent neural network for skeleton-based dynamic hand gesture recognition," in Proc. Int. Conf. Image Process. (ICIP), Beijing, China, Sep. 2017, pp. 2881–2885.
- [113] M. Maghoumi, JJ. LaViola Jr. DeepGRU: Deep Gesture Recognition Utility. In arXiv preprint arXiv:1810.12514, 2018
- [114] Q. Oliveau and H. Sahbi. "Semi-supervised deep attribute networks for fine-grained ship category recognition." In IGARSS 2018-2018 IEEE International Geoscience and Remote Sensing Symposium, pp. 6871-6874. IEEE, 2018.
- [115] J. Liu, G. Wang, L. Duan, K. Abdiyeva, and A. C. Kot. Skeleton-based human action recognition with global context-aware attention lstm networks. *IEEE Transactions on Image Processing*, 27(4):1586–1599, April 2018
- [116] J. Liu, A. Shahroudy, D. Xu, and G. Wang. Spatio-temporal LSTM with trust gates for 3D human action recognition. In European Conference on Computer Vision, pages 816–833. Springer, 2016
- [117] H. Sahbi. "Learning cca representations for misaligned data." In Proceedings of the European Conference on Computer Vision (ECCV) Workshops, pp. 0-0. 2018.
- [118] J. Wang, Z. Liu, Y. Wu, and J. Yuan. Mining Actionlet Ensemble for Action Recognition with Depth Cameras. In CVPR, pages 1290–1297, 2012.
- [119] X. Yang and Y. Tian. Effective 3D action recognition using eigenjoints. *Journal of Visual Communication and Image Representation*, 25(1):2–11, 2014.
- [120] Q. Oliveau and H. Sahbi. "Semantic-free attributes for image classification." In 2016 23rd International Conference on Pattern Recognition (ICPR), pp. 1577-1582. IEEE, 2016.